Angular momentum regulation strategies for highly dynamic landing in Parkour

Galo Maldonado, François Bailly, Philippe Souères, Bruno Watier

Angular momentum regulation strategies for highly dynamic landing in Parkour

Galo Maldonado*†, François Bailly*†, Philippe Souères* and Bruno Watier*†
*LAAS, CNRS, Toulouse, France
†LAAS, University of Toulouse, UPS, Toulouse, France
Email corresponding author: galo.maldonado@laas.fr

***Abstract*—Previous studies have shown that angular momentum is regulated during daily life activities like walking and during dynamic motions such as somersaults and twists. In this paper, we propose to extend these works by studying how the regulation of the angular momentum derivative *AMD* contributes to mechanical stability after a highly dynamic drop. To this end, five healthy Parkour experts participated in this study and were asked to perform the Parkour precision landing technique. The derivative of angular momentum expressed at the center of mass position and the contribution of each segment to its variation were analyzed. Results show that the *AMD* is regulated to zero throughout landing. Our study also reveals complex whole-body strategies of Parkour practitioners such as opposed segment cancellations and a temporal organization of the motion. This study provides a new basis to better understand dynamic landing performances. Results could also be used to generate landing motions with humanoid robots or virtual avatars (human-inspired motion).**

I. Introduction

Angular momentum was shown to be regulated during daily life activities such as walking [1] or during more complex motions (also observed in Parkour and freerunning) like somersaults and twists [2]. In [1] it was suggested that during gait, segment-to-segment angular momentum cancellations regulate the total angular momentum expressed at the CoM position and that active generation of angular momentum is a key strategy for bipedal manoeuvrability and stability. According to Euler's second law of motion, the derivative of the angular momentum (*AMD*) expressed at the CoM position is equal to the sum of the external net torques applied to the body. This quantity can be regulated by humans when contacting the ground at landing to maintain equilibrium and avoid tipping motions [3]. In relatively recent studies, information from angular momentum observed in human movements has been transferred to anthropomorphic avatars [4] and the control of bipedal robots [5], [6].

Motivated by these studies, we propose to conduct a whole-body biomechanical study by analyzing the *AMD* expressed at the CoM in Parkour precision landings performed by Parkour experts. We hypothesize that traceurs regulate the *AMD* among the three principal axis of rotation to achieve stability in such a dynamic motion as precision landing. To extend our analysis, we also study postural control strategies by looking into segmental contributions to the total *AMD* expressed at the CoM position.

II. Methodology

A. Participants

Five healthy trained male traceurs (age: 22.2 ± 4.8 y, height: 1.73 ± 0.04 m, mass: 66.6 ± 5.1 kg) volunteered for the study. The traceurs' experience in Parkour practice was 5.4 ± 2.1 years. The subject exclusion criterion was based on history of lower extremity injuries or diseases that might affect jump and landing biomechanics. The experiments were conducted in accordance with the standards of the Declaration of Helsinki (rev. 2013) and approved by a local ethics committee.

B. Experimental protocol

Participants performed a warming up session followed by a familiarization period during which the protocol instructions were provided to them, and during which they familiarized with the lab environment. The landing protocol was designed to include a jump height of 75% of the height of the participant and a landmark placed at a distance equal to the square of the jump height. For setting-up the protocol, a tubular structure used for Parkour training was modified and assembled according to the design shown in Fig. 1. During the recording protocol, participants were asked to land onto the target specified by landmarks on each force plate using the Parkour precision technique.

C. Data acquisition

A total of 8 successful repetitions per participant was recorded. 3D whole-body kinematic data were collected using 14 infra-red cameras sampling at 400 Hz (Vicon, Oxford Metrics, Oxford, UK) and recording 48 reflective markers placed on the participant's body. Markers were located on the participants' body based on Wu and Dumas recommendations [7]–[10] as follows: the first, and fifth metatarsal, second toe tip, calcaneus, lateral and internal malleolus, anterior tibial tuberosity, lateral and medial epicondyles of knee, greater trochanter, posterior superior iliac spine and anterior superior iliac spine, procesuss xiphoideus, incisura jugularis, seventh cervicale, tenth thoracic vertebra, acromioclaviculare, medial and lateral epicondyle, ulnar and radial styloid, second and fifth metacarpal heads, second fingertip, sellion, occiput, right and left temporal. Two force plates (AMTI, Watertown, MA, USA) embedded into the floor in order to record landing GRFs and two rigid handle bar sensors (SENSIX, Poitiers,Vienne, France) with a diameter of 63 mm were used sampling at 2000 Hz. Handle bar sensors were placed on a Parkour tubular structure to record take-off GRFs. Force data were used to define the onsets dividing the Parkour motion into phases.

D. Data analysis

Kinematics and kinetics were processed with the same cut-off frequency [11] using a low-pass Butterworth digital filter of 4th order applied in a zero-phase. A cut-off frequency of 35 Hz was used after a residual analysis [12]. The score method was used to better estimate the center of hip and shoulder joints [13].

Inverse kinematics was solved by minimizing the squared distance between recorded and virtual markers (global optimization method [14]) using OpenSim software with a whole-body skeletal model. All momenta computations were performed using a custom made program with a whole-body model and a physics engine [15]. Kinematic and anthropometric data were merged to compute the *AMD* contribution of each segment k expressed at the CoM position according to the following equation:

$$\dot{\mathcal{L}}_k = I_k\dot{\omega} + \omega_k \times (I_k\omega), \tag{1}$$

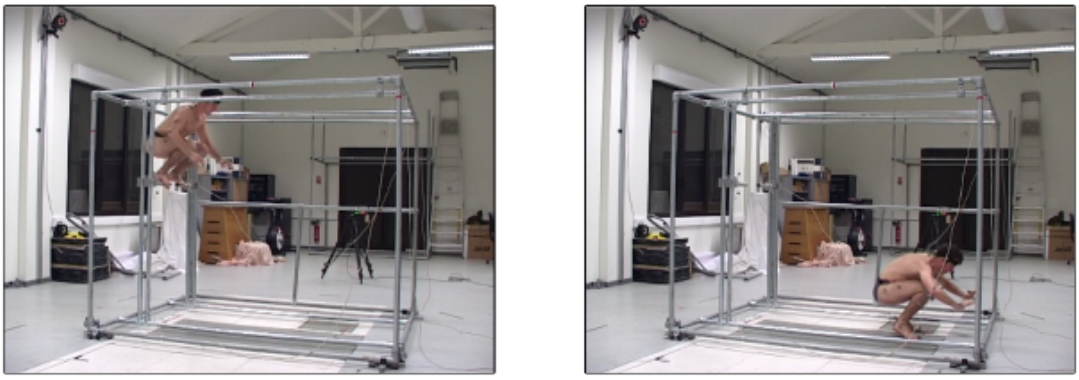

(a) **(b)**

Fig. 1: Parkour precision jump (**a**) and landing (**b**) techniques performed inside a motion capture laboratory. Only the landing phase was used in the analysis of the angular momentum derivative.

where I_k is the inertia matrix of the k^{th} segment, ω_k is the angular velocity of the k^{th} segment, each expressed in the inertial frame (CoM) of the segment. Using Eq. (1), individual contribution of segments was expressed at the CoM and summed in order to analyze the whole body postural control strategy.

The motion was divided into three phases: take-off, flight, and landing. The take-off phase was defined from the minimum vertical position of the CoM until the last foot contact. The flight phase was defined between the end of the take-off phase until the initial contact "IC" with the ground, that we identified as the instant when the vertical ground reaction force reached 50 N, and the landing phase was defined from IC until the CoM reached its minimum vertical position. Each phase was normalized by its time duration from 0% to 100%. The linear momentum was normalized by the participant weight, and the angular momentum was normalized by the participant weight and height. Mean and standard deviation were calculated for each participant and for the whole group.

E. Skeletal Model

A whole-body 3D model including 42 degrees of freedom and 19 segments was used to reconstruct the main elementary movements of the Parkour athlete. The main characteristics of the model are listed below:

- The lower limbs, pelvis and upper limb anthropometry are based on the running model of Hammer et al. [16]. Mass properties of the torso and head segments (including the neck) are estimated from the regression equations of ([7], [8]. Hands anthropomorphic data are based on regression equations [17].
- Each lower extremity has 7 DoF. The hip is modeled as a ball-and-socket joint, the knee is modeled as a hinge joint, the ankle is modeled as 2D hinge joints (flexion-extension and inversion-eversion), and the toes are modeled with one hinge joint at the metatarsals.
- The pelvis joint is modeled as a free-flyer joint to permit the model to translate and rotate in the 3D space. This 6D joint is attached to the free-floating base (root frame) of the under-actuated system. The lumbar motion is modeled as a ball-and-socket joint [18] and the neck joint is also modeled as a ball-and-socket joint.
- Each arm is modeled with 8 DoF. The shoulder is modeled as a ball-and-socket joint, the elbow and forearm rotations are modeled as hinge joints to represent flexion-extension and pronation-supination [19], the wrist flexion-extension and radial-ulnar deviations are modeled as hinge joints, and the hand fingers are modeled as one hinge joint for all fingers.

III. Results

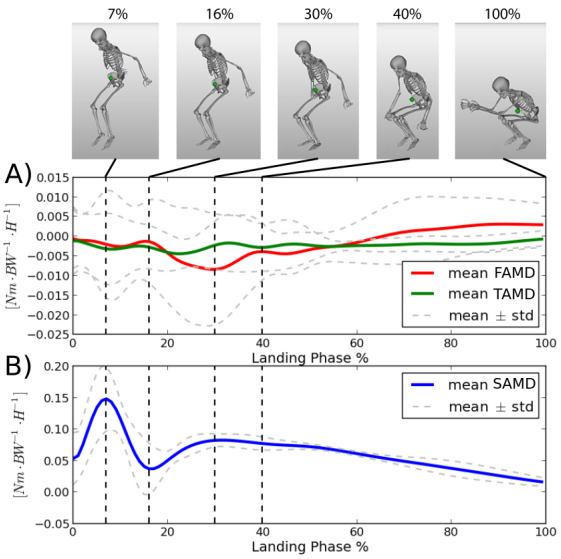

Fig. 2: Mean (±std) of the *AMD*. In (**A**, red), the frontal *AMD* around A-P axis "FAMD". In (**A**, green), the transversal *AMD* around vertical axis "TAMD". In (**B**, blue), sagittal *AMD* around M-L axis "SAMD". In the top, snapshots of representative configurations extracted from the inverse kinematics computation, of a participant executing the precision landing technique.

The three components of the *AMD* vector were labelled as "FAMD", "SAMD" and "TAMD". *AMD* was normalized by the height and the body weight of each participant. Regulation to zero of the 3 components of the *AMD* was observed (Fig. 2). A recurrent segment cancellation strategy is revealed (Fig. 3). It appears that at

the beginning of the landing phase, pelvis, torso and head are not used for stabilization while upper and lower limbs work together to regulate the *AMD*. Small adjustments of total *AMD* at the CoM were observed in the end of the motion by upper limbs at the frontal and transversal planes.

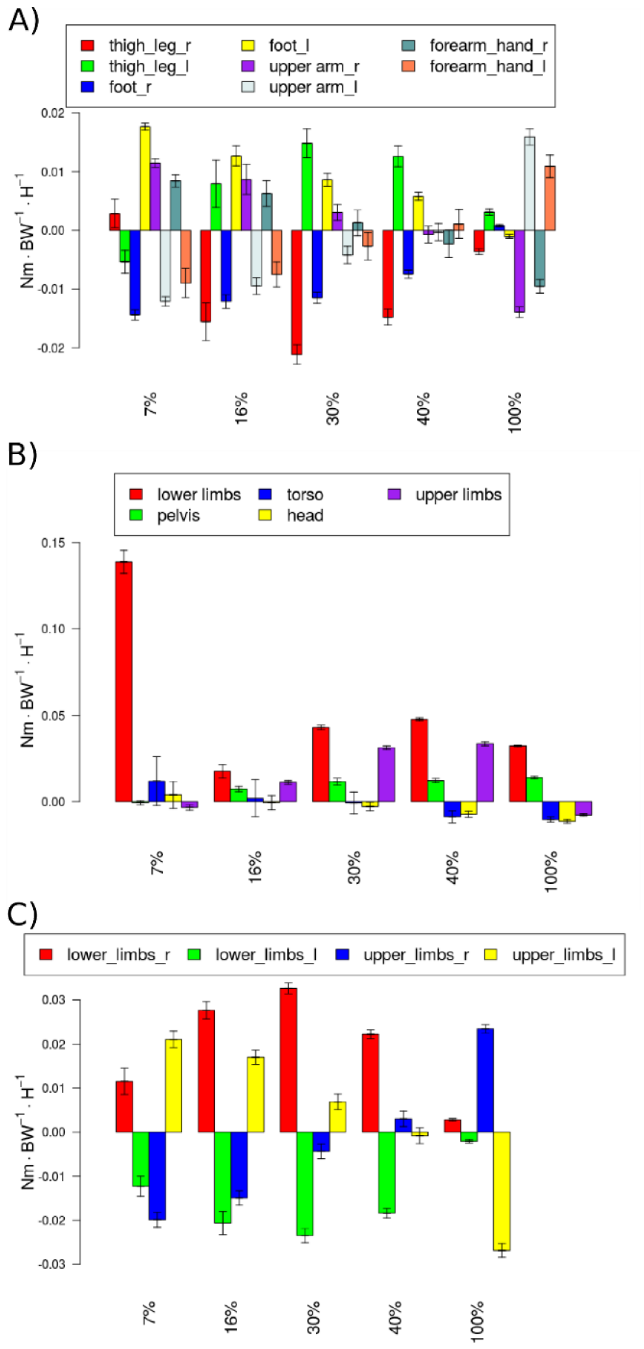

Fig. 3: Segment groups contribution to total *AMD*. In (**A**), contributions to FAMD. In (**B**), contribution to SAMD. In (**C**), contributions to TAMD. Angular momentum derivative is normalized by the height and body weight. The time is normalized from 0% to 100%

IV. Discussion

The derivative of angular momentum (*AMD*) appears to be minimized by the mechanical actions of whole-body segments during Parkour precision landing (Fig. 2B). This make sense as the *AMD* expressed at the CoM is directly linked to the body's angular acceleration, according to Euler's law. Our study also reveals complex strategies of traceurs such as opposed segment cancellations and temporal organization of the motion.

A. Frontal AMD around A-P axis "FAMD"

FAMD is regulated around zero with small variations ($\pm 0.01 Nm \cdot BW^{-1} \cdot H^{-1}$). A strategy of right and left segments cancellation is observed (Fig. 3) which contributes to minimize the FAMD. In the beginning of the landing phase (up to 40 %), the control comes from lower limbs contribution especially. This might be a strategy of the jumper to prevent injuries such as ACL or sprains by avoiding excessive varus-valgus motions. Furthermore, an important segment cancellation of the arms at the end of the motion phase is observed. It seems that this is a potential error correction strategy that insures the final regulation to zero of the FAMD. This might be linked to the fact that the traceur has almost reached the lower limb's joint limits and therefore needs another strategy to control FAMD. This is why the traceur chooses to use the arms which are free to move to compensate the small deviation.

B. Sagittal AMD around M-L axis "SAMD"

Fig. 2 reveals a perturbation rejection profile of the SAMD (up to 40% of the movement) where the lower limbs contribution at the beginning of the landing phase is considerable. This is not surprising as the main tipping effects occur in the sagittal plane after a standing long jump.

C. Transversal AMD around vertical axis "TAMD"

TAMD is regulated around zero with small variations ($\pm 0.02 Nm \cdot BW^{-1} \cdot H^{-1}$). The same segment cancellation strategy as in FAMD is used to minimize the *AMD* in the transversal plane. The upper limbs segment cancellation is important at the end of the phase and the same reasoning as for FAMD applies.

D. Segment cancellation interpretation

At first glance, inter-segment cancellation does not contribute to *AMD* of angular momentum. We interpret it in terms of an energy storing strategy for potential mechanical action to control stability. Potential, because if the motion stays symmetrical, the contribution is null, otherwise, the inter-segment difference generates the required torque at the CoM. In this way, the mechanical action can be generated precisely and instantaneously (by making profit of the motion dynamics) instead of producing it from scratch.

V. Conclusions

In this study, a whole-body analysis of angular momentum during Parkour precision landing was presented. It is interesting to highlight that whole-body dynamic strategies to regulate the *AMD* at the CoM to zero were observed. This might serve as a starting point to test if performance variables linked to angular momentum are being controlled steadily by the brain. This study provides also a basis for better understanding dynamic landing performances and for generating such motions with anthropomorphic systems such as humanoid robots or virtual avatars (human-inspired motion).

Acknowledgments

Part of this work is supported by ANR Entracte project (ANR 13CORD-002-346 01) and the European Research Council for the project Actanthrope (ERC-ADG347 340050).

REFERENCES

[1] H. Herr and M. Popovic, "Angular momentum in human walking." *The Journal of experimental biology*, vol. 211, no. Pt 4, pp. 467–81, mar 2008. [Online]. Available: http://www.ncbi.nlm.nih.gov/pubmed/18245623

[2] C. Frohlich, "Do spring board divers violate angular momentum conservation?" *American Journal of Physics*, vol. 47, no. 7, pp. 583–592, 1979.

[3] P. Sardain and G. Bessonnet, "Forces Acting on a Biped Robot. Center of Pressure—Zero Moment Point," *IEEE Transactions on Systems, Man, and Cybernetics - Part A: Systems and Humans*, vol. 34, no. 5, pp. 630–637, sep 2004. [Online]. Available: http://ieeexplore.ieee.org/lpdocs/epic03/wrapper.htm?arnumber=1325327

[4] a. Hofmann, M. Popovic, and H. Herr, "Exploiting angular momentum to enhance bipedal center-of-mass control," *2009 IEEE International Conference on Robotics and Automation*, pp. 4423–4429, may 2009. [Online]. Available: http://ieeexplore.ieee.org/lpdocs/epic03/wrapper.htm?arnumber=5152573

[5] S. Yun and A. Goswami, "Momentum-based reactive stepping controller on level and non-level ground for humanoid robot push recovery," in *2011 IEEE/RSJ International Conference on Intelligent Robots and Systems*, Sept 2011, pp. 3943–3950.

[6] A. Goswami and V. Kallem, "Rate of change of angular momentum and balance maintenance of biped robots," in *Robotics and Automation, 2004. Proceedings. ICRA '04. 2004 IEEE International Conference on*, vol. 4, April 2004, pp. 3785–3790.

[7] R. Dumas, L. Chèze, and J. P. Verriest, "Adjustments to mcconville et al. and young et al. body segment inertial parameters," *Journal of Biomechanics*, vol. 40, no. 3, pp. 543–553, 2007.

[8] R. Dumas, L. Chèze, and J.-P. Verriest, "Corrigendum to "Adjustments to McConville et al. and Young et al. body segment inertial parameters" [J. Biomech. 40 (2007) 543–553]," *Journal of Biomechanics*, vol. 40, no. 7, pp. 1651–1652, 2007. [Online]. Available: http://linkinghub.elsevier.com/retrieve/pii/S0021929006002740

[9] G. Wu, S. Siegler, P. Allard, C. Kirtley, A. Leardini, D. Rosenbaum, M. Whittle, D. D. D'Lima, L. Cristofolini, H. Witte, O. Schmid, and I. Stokes, "ISB recommendation on definitions of joint coordinate system of various joints for the reporting of human joint motion—Part I: ankle, hip, and spine," *Journal of Biomechanics*, vol. 35, no. 4, pp. 543–548, 2002. [Online]. Available: http://linkinghub.elsevier.com/retrieve/pii/S0273230002915497

[10] G. Wu, F. C. van der Helm, H. (DirkJan) Veeger, M. Makhsous, P. Van Roy, C. Anglin, J. Nagels, A. R. Karduna, K. McQuade, X. Wang, F. W. Werner, and B. Buchholz, "ISB recommendation on definitions of joint coordinate systems of various joints for the reporting of human joint motion—Part II: shoulder, elbow, wrist and hand," *Journal of Biomechanics*, vol. 38, no. 5, pp. 981–992, 2005. [Online]. Available: http://linkinghub.elsevier.com/retrieve/pii/S002192900400301X

[11] E. Kristianslund, T. Krosshaug, and A. J. Van den Bogert, "Effect of low pass filtering on joint moments from inverse dynamics: Implications for injury prevention," *Journal of Biomechanics*, vol. 45, no. 4, pp. 666–671, 2012. [Online]. Available: http://dx.doi.org/10.1016/j.jbiomech.2011.12.011

[12] D. A. Winter, *Biomechanics and motor control of human movement, Fourth Edition*. John Wiley & Sons, Inc, 2009.

[13] R. M. Ehrig, W. R. Taylor, G. N. Duda, and M. O. Heller, "A survey of formal methods for determining the centre of rotation of ball joints," *Journal of Biomechanics*, vol. 39, no. 15, pp. 2798–809, 2005. [Online]. Available: http://www.ncbi.nlm.nih.gov/pubmed/16293257

[14] T.-W. Lu and J. O'Connor, "Bone position estimation from skin marker co-ordinates using global optimisation with joint constraints," *Journal of Biomechanics*, vol. 32, no. 2, pp. 129 – 134, 1999. [Online]. Available: http://www.sciencedirect.com/science/article/pii/S0021929098001584

[15] J. Carpentier, F. Valenza, N. Mansard, and Others, "Pinocchio: fast forward and inverse dynamics for poly-articulated systems," https://stack-of-tasks.github.io/pinocchio, 2015.

[16] S. R. Hamner, A. Seth, and S. L. Delp, "Muscle contributions to propulsion and support during running," *Journal of Biomechanics*, vol. 43, no. 14, pp. 2709–2716, 2010.

[17] P. D. Leva, "Adjustements to Zatsiorsky-Seluyanov's segment inertia paremeters," *Journal of Biomechanics*, vol. 29, no. 9, pp. 1223–1230, 1996.

[18] F. C. Anderson and M. G. Pandy, "A Dynamic Optimization Solution for Vertical Jumping in Three Dimensions," *Computer Methods in Biomechanics and Biomedical Engineering*, vol. 2, no. 3, pp. 201–231, 1999. [Online]. Available: http://dx.doi.org/10.1080/10255849908907988

[19] K. R. S. Holzbaur, W. M. Murray, and S. L. Delp, "A Model of the Upper Extremity for Simulating Musculoskeletal Surgery and Analyzing Neuromuscular Control," *Annals of Biomedical Engineering*, vol. 33, no. 6, pp. 829–840, 2005. [Online]. Available: http://dx.doi.org/10.1007/s10439-005-3320-7